

Measurement of the bending stiffness of masonry walls by using time-frequency analysis: Practical considerations and validation

Charlotte CRISPIN¹; Christian MERTENS

¹ Belgian Building Research Institute, Belgium

ABSTRACT

The bending stiffness is one of the parameters that determines the mechanical behaviour of a plate and therefore influences the acoustic performance of building elements. Besides, it appears in the prediction models for calculating the sound reduction index, R , or recently the vibration reduction index, K_{ij} . Its accurate determination is thus essential in the field of acoustics. The Atomic Energy Research Institute of Korea has proposed an interesting measurement technique to determine this parameter in-situ. This technique, which uses the time-frequency analysis, has been successfully applied to thin plates. However, this paper shows that corrections should be used for thick walls. Some practical considerations are given and some measurements results for masonry walls are presented.

Keywords: Material, Properties, Bending

1. INTRODUCTION

The vibratory analysis of a plate excited by a hammer hit shows that quasi-longitudinal waves (symmetric zero order mode, S_0 , of the Lamb waves) and bending waves (Anti-symmetric zero order mode, A_0 , of the Lamb waves) can settle in it. This article focuses on those latter. Indeed, they can be used to determine the dynamic properties of the plates.

The traveling velocity of the bending waves depends on the dynamic properties of the wall but also depends on the frequency: the bending waves are said to be dispersive. This means that the high frequency bending waves are faster than the low frequency.

The measurement of the traveling velocity of the bending wave's energy and the adjustment of the results on a theoretical curve lead to the determination of the interdependent dynamic properties of plates.

For thin plates, the traveling velocity of the bending wave's energy is easily measured with accelerometers and the well-known relationships between the dynamic properties can be used without special precautions. For thicker plates, the relevant signal is more difficult to obtain, and the simplified formulas dedicated to the thin plates are no longer valid.

2. RELATIONSHIP BETWEEN THE DYNAMIC PROPERTIES

2.1 For thin plate

In most books on acoustics, the relationships between the dynamic properties of the plates, which are proposed, are based on the theory for thin plates and are given by the well-known following formulas:

$$C_{g,thin} \approx 2\sqrt{1.8c'_L hf} \quad (1)$$

$$f_c = \frac{c_0^2 \sqrt{3}}{\pi h c'_L} \quad (2)$$

¹ Charlotte.crispin@bbri.be

And,

$$B = \frac{c_0^4 \rho h}{4\pi^2 f_c^2} \quad (3)$$

With,

$C_{g,thin}$, the group velocity of the bending waves according to the thin plate theory;
 h , the thickness of the plate [m];
 f , the frequency [Hz];
 c'_L , the quasi-longitudinal wavespeed [m/s]
 ρ , the density of the plate [kg/m³];
 B , the bending stiffness [Nm];
 f_c , the critical frequency [Hz];
 c_0 , the wavespeed in air [m/s]

Traditionally, the limit for the applicability of these formula is given by Cremer (1):

$$\lambda_B \geq 6h \quad (4)$$

At high frequencies, additional terms need to be added to take account the shear deformations and the rotary inertia (2). These corrections result in a bending wavespeed that is lower than that given by the equation for pure bending wave and the above equations are no longer valid.

2.2 For thick plate

In his article, Rindel (3) presents an equation for the effective phase speed, c_{ph} , in a thick plate. This equation is a combination of bending and shear waves. The representation of this function as a function of frequency shows at high frequency a convergence towards an asymptote given by the shear wavespeed, c_s , which cannot be accurately determined. Ross (4) proposes another formula. According to him, in a uniform and monolithic plate, the phase velocity of the bending wave can be approximated by:

$$c_{ph,Ross} = c'_L \sqrt{\frac{1.8hf}{c'_L + 4.5hf}} \quad (5)$$

And the group velocity is given by:

$$C_{g,Ross} = \frac{3.6hf c'_L{}^2}{c_{ph,Ross}(c'_L + 9hf)} \quad (6)$$

The adjustment of this theoretical curve on a measured group velocity curve gives the quasi-longitudinal wavespeed c'_L .

For masonry walls, the critical frequency is low enough to use the thin plate theory for its determination and for the calculation of the bending stiffness, B , according to Eq.2 and Eq.3 respectively.

3. THE EXPERIMENTAL PROCEDURE FOR MEASURING THE TRAVELING VELOCITY OF THE EFFECTIVE BENDING WAVE'S ENERGY

Different techniques were tested to measure the bending wavespeed or the longitudinal wavespeed (4, 5, 6, 8) in thick plates. In this article, it is the traveling velocity of the bending wave's energy (the group velocity) which is determined and which is used for the calculation of the c'_L .

In their article, Y-C. Choi and Cie (7) present a suitable method to determine the group velocity of the bending waves by using a time-frequency analysis. The group velocity equals the distance between two accelerometers divided by the time delay between these accelerometers. Being dispersive, the group velocity must be given as a function of the frequency.

$$C_g(f) = \frac{\Delta x}{\Delta t(f)} \quad (7)$$

Where,

Δt is the arrival time delay of the bending wave's energy according to the frequency between two accelerometers;

Δx is the distance between these two accelerometers.

The arrival time delay between the accelerometers is obtained by the Wigner-Ville analysis. This analysis allows to obtain the energy distribution of a short signal as a function of time and of frequencies. The approach of Wigner-Ville is based on the instantaneous autocorrelation function and is defined as (9):

$$W_s(t, \omega) = \frac{1}{2\pi} \int s\left(t + \frac{\tau}{2}\right) s^*\left(t - \frac{\tau}{2}\right) e^{-j\omega\tau} d\tau \quad (8)$$

Thus, with this time-frequency analysis method, the arrival time delay can be obtained at each frequency with a very good time resolution.

The adjustment of the theoretical curve of $C_{g,Ross}$ [Eq. 6] on the measured group velocity curve [Eq. 7] provides then the quasi-longitudinal wave velocity c'_L .

4. EXPERIMENTAL RESULTS

4.1 Aluminium plate

A hammer hit is applied on a suspended aluminium plate with the dimensions 1.45 m x 1.35 m x 0.0025 m (figure 1). The density of the plate is 2153 kg/m³. Two accelerometers are spaced of 0.1 m and the impact is given at 0.15 m from the accelerometer 1 on the same line. The signals are recorded by a data acquisition system with a sample frequency of 192000Hz.



Figure 1 – Picture of the Aluminium plate

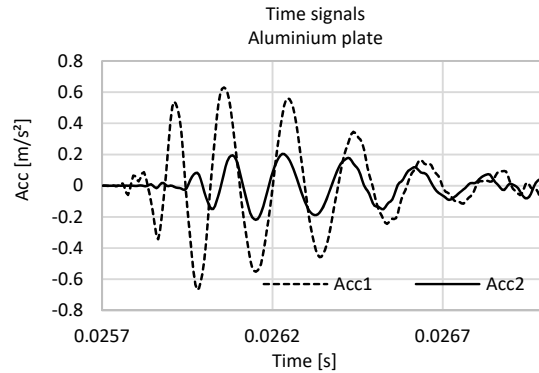


Figure 2 – Time signals for the two accelerometers

Figure 2 shows the acceleration signals of the two accelerometers. The Wigner-Ville analysis applied to both signals gives their frequency distribution of the energy as a function of time (figure 3). As expected, and according to the dispersion law of the bending waves, the highest frequencies arrive first followed by the medium frequencies and finally by the lowest frequencies. On these graphs, the peak magnitudes of the energy distributions are gathered (red curves). The two curves are then displayed on the same graph (Figure 4) in order to determine the time delay at each frequency.

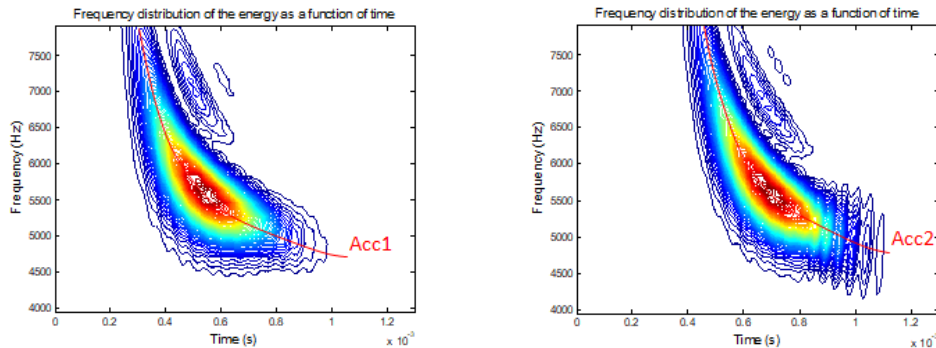


Figure 3 – Frequency distribution of the energy as a function of time for the two accelerometers

The group velocity can be then calculated by applying [Eq.7]. The determination of the first dynamic property, the quasi-longitudinal wavespeed, c'_L , is reached by the adjustment of the theoretical curve $C_{g,Ross}$ [Eq. 6]. The results are shown figure 5. The $C_{g,thin}$ [Eq.1] of the thin plate theory is also presented in this figure.

For the aluminium plate, the thin plate theory gives nearly the same results than the thick plate theory and the relationships Eq 1 to Eq 3 can be used for the determination of the dynamic properties.

The calculated quasi-longitudinal wavespeed, c'_L , is 3632 m/s; the critical frequency, f_c , is 7019 Hz and the bending stiffness, B , is 37 Nm,.

This procedure was also successfully applied for the determination of the properties of the plasterboards.

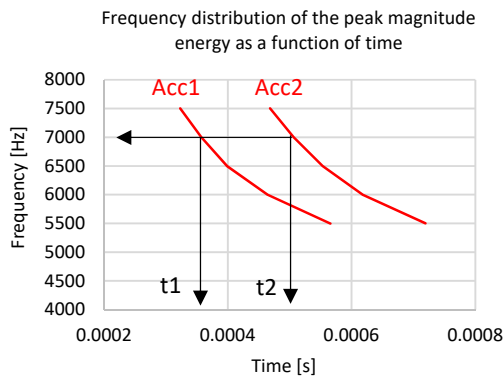


Figure 4 – Frequency distribution of the peak energy as a function of time for the two accelerometers

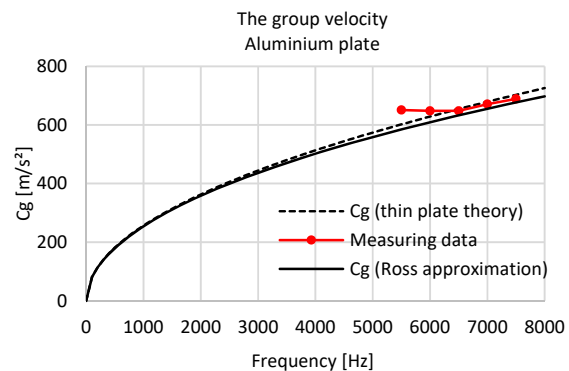


Figure 5 – The measured group velocity compared to the theoretical expressions

4.2 Gypsum block walls

The wall is composed of gypsum blocks (figure 6). Its dimensions are 2.4m x 4m and the thickness is 0.07 m. The block density is 1066 kg/m³.

This partition wall is in fact a composition of a double wall for which the airborne sound insulation was measured (figure 7). The result of this test is important because it shows us that the critical frequency falls in the third octave band of 500 Hz. This data will allow us to validate our results.

For this case, a horizontal line of 8 accelerometers spaced of 0.05 m is used. The impact is given at 0.10 m from the accelerometer 1 on the same line. The averaged time delay obtained between all of these accelerometers gives a best accuracy on the results.

The signals are recorded by a data acquisition system with a sample frequency of 204800Hz.



Figure 6 – Picture of the gypsum block wall and the horizontal line of accelerometers

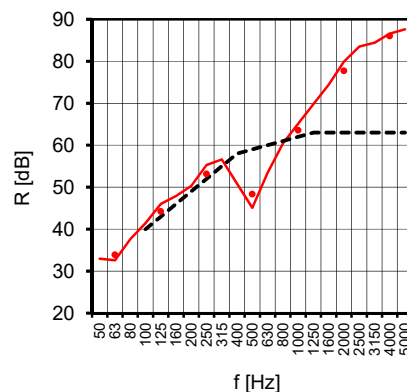


Figure 7 – The sound reduction index of the double gypsum wall

The exploitable signals are in the first milliseconds because the standing waves set in very quickly. A time window is then used to isolate the relevant signals. A low-pass and a high-pass filters are also applied. The frequency range of interest is that which gives the wavelengths between $3h$ and $L/3$ (where h is the thickness and L , the width of the walls). In this case:

$$0.21 \text{ m} < \lambda_{interest} < 0.8 \text{ m}$$

Or,

$$400 \text{ Hz} < f_{interest} < 5000 \text{ Hz}$$

A hammer with a hard head is used to give sufficient energy in this frequency range. Figure 8 gives the Wigner-Ville analysis for the first four accelerometers. The distribution curve appears quite clearly on the graphs.

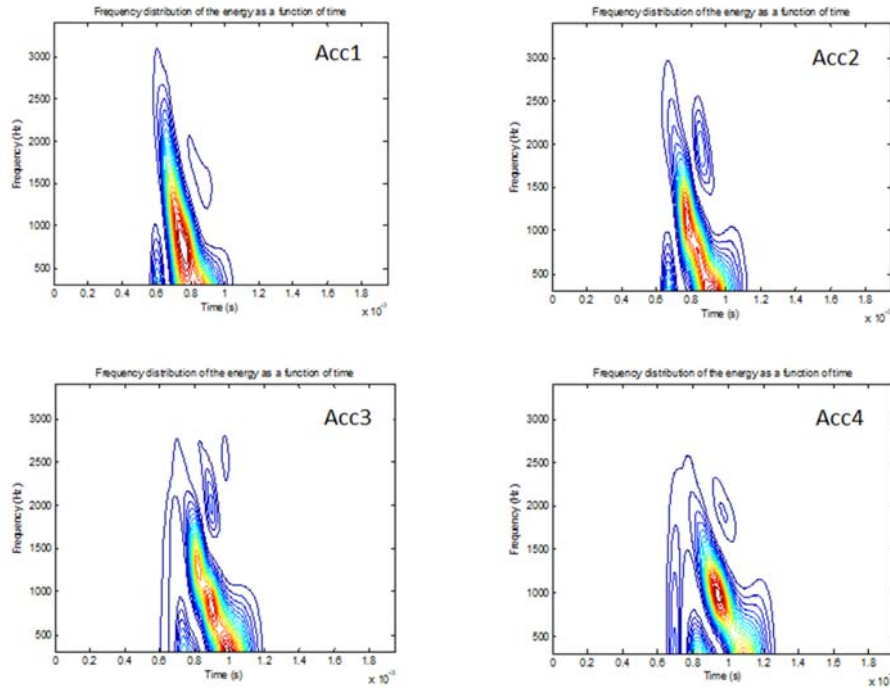


Figure 8 – Frequency distribution of the energy as a function of time for the first four accelerometers aligned horizontally

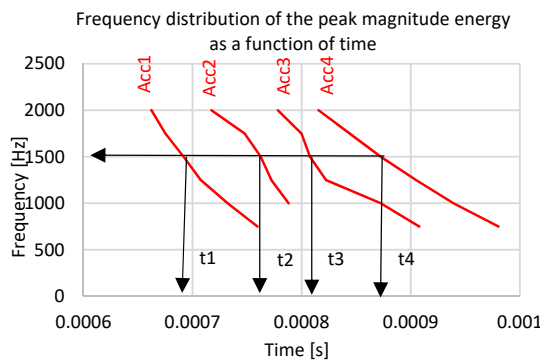


Figure 9 – Frequency distribution of the peak energy as a function of time for the first four accelerometers aligned horizontally

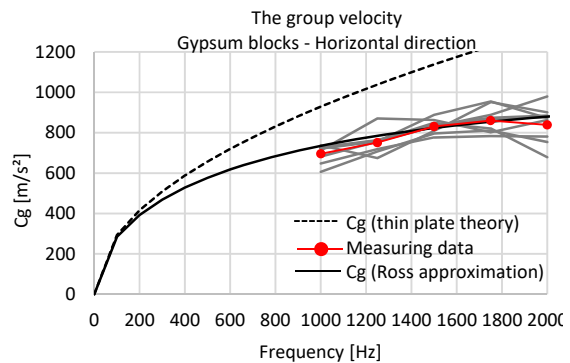


Figure 10 – The measured group velocity compared to the theoretical expressions for the horizontal direction

The peaks of the bending wave energy of each graphs are gathered and they are presented on the same graph (figure 9). At each frequency, the group velocity is evaluated between different

accelerometers. The light grey curves show these results on figure 10. The red curve represents the average of these curves. The adjustment of the theoretical curve according the thin plate theory gives inconsistent results because this plate can no longer be considered as a thin plate.

The adjustment of the $C_{g,Ross}$ gives: $c'_L \approx 1699$ m/s. The calculated f_c , according to Eq. 2, is then 536 Hz and the bending stiffness is $B=87958$ N.m;

This critical frequency falls in the third octave band of 500 Hz observed on the spectrum of sound reduction index, R (figure 7).

The figures below present the results for the vertical direction. The adjustment of the $C_{g,Ross}$ (figure 13) gives: $c'_L \approx 1867$ m/s. The calculated f_c is then 488 Hz and the bending stiffness is $B=106156$ N.m;

This critical frequency falls yet in the third octave band of 500 Hz observed on the spectrum of sound reduction index, R .

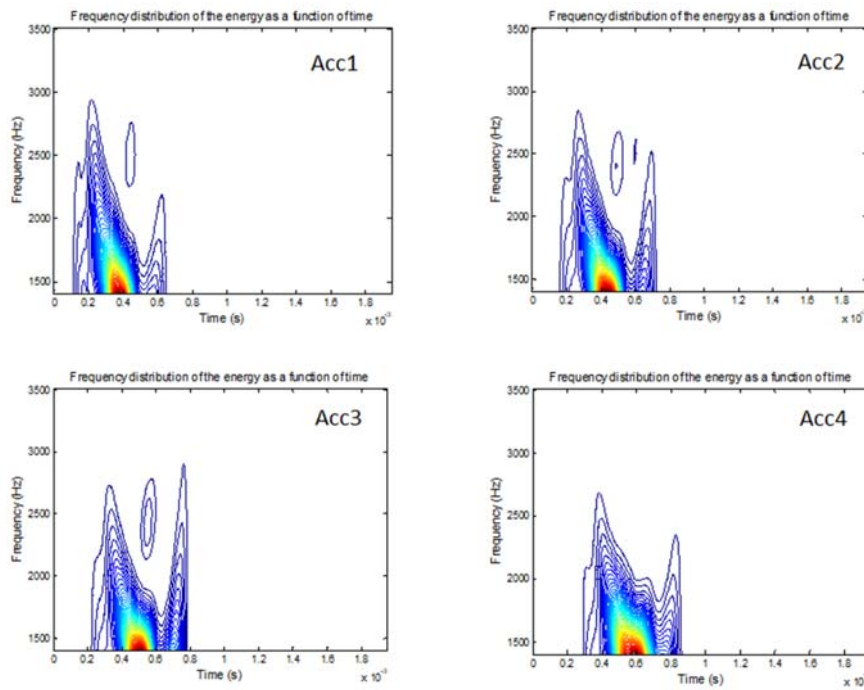


Figure 11 – Frequency distribution of the energy as a function of time for the first four accelerometers aligned vertically

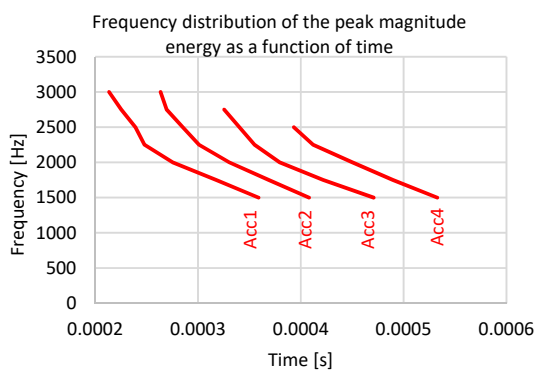


Figure 12 – Frequency distribution of the peak magnitude energy as a function of time for the first four accelerometers aligned vertically

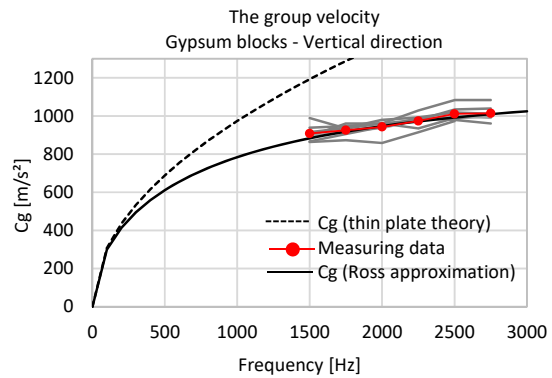


Figure 13 – The measured group velocity compared to the theoretical expressions for the vertical direction

4.3 Brick wall

This procedure was also tested for a wall composed of perforated bricks (h is 0.14 m and ρ is 900 kg/m³) and with the same dimensions than the gypsum block wall. The results are summarised at figures 15 and 16 only for the diagonal direction. The measurements were carried out on the plastered wall (Figure 14).



Figure 14 – Picture of the brick wall and the diagonal line of accelerometers

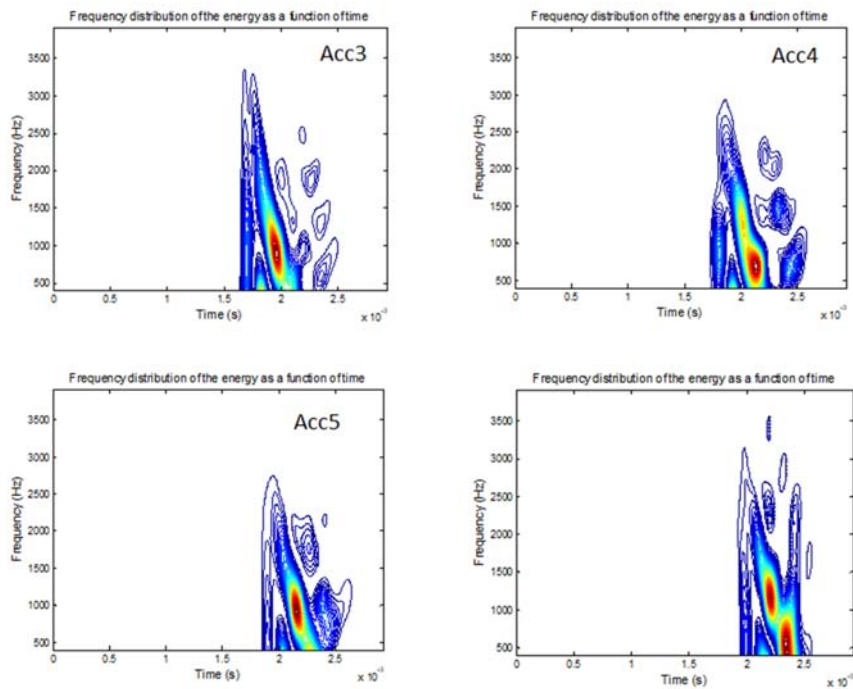


Figure 15 – Frequency distribution of the energy as a function of time for the first four accelerometers aligned diagonally

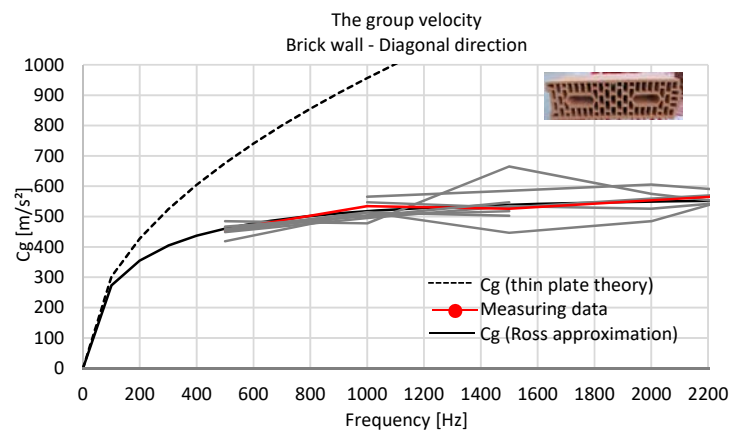


Figure 16 – Frequency distribution of the peak energy as a function of time for six accelerometers

The adjustment of the $C_{g,Ross}$ (figure 16) on the results gives: $c'_L \approx 900$ m/s. The calculated f_c , is then 506 Hz and the bending stiffness is $B=166736$ N.m. This estimated f_c is consistent with the result obtained on the spectrum of the sound reduction index.

The procedure described here for the determination of the dynamic properties is applicable as long as the size of the inhomogeneities (the size of the holes in the blocks) is small compared to generated wavelengths.

5. CONCLUSIONS

The adjustment of a theoretical curve of the group velocity, C_g , on measurement results allows to obtain the dynamic properties of masonry walls. The theoretical expression of C_g coming from the thin plate theories gives aberrant results because the masonry walls are relatively thick compared to the wavelength of the structural waves and they exhibit more complicated dispersions than thin plate. It is the Ross's approximation which is more relevant for thick plate, that should be used to estimate theoretically C_g and c_{ph} .

Experimentally, the group velocity is reached by the measurement of the arrival time delay of the bending wave's energy according to the frequency between two accelerometers whose the distance that separate them is known. This is the Wigner-Ville analysis, which is used to obtain, with relatively good accuracy, these arrival time delays. Practically, the exploitable signals for masonry walls, are in the first milliseconds because the standing waves set in very quickly. A time window is then used to isolate the relevant signals. A low-pass and a high pass filters are also applied.

This procedure is applicable as long as the size of the inhomogeneities in the masonry blocks is small compared to generated wavelengths.

ACKNOWLEDGEMENTS

This study was done in the framework of the project A-light II (Integrating lightweight concepts in acoustical standardization). The authors are grateful for the financial support from the Federal Public Service Economy of Belgium.

REFERENCES

1. Cremer L., Heckl M. and Ungar E.E. Structure-borne Sound: Structural Vibrations and Sound at Audio Frequencies, 2nd edn. Springer-Verlag New York Heidelberg Berlin, 1988.
2. Mindlin R.D. (1951) Influence of Rotary Inertia and Shear on Flexural Motions of Isotropic, Elastic Plates, *Journal of Applied Mechanics*, Vol.18,pp. 31-38.
3. Rindel J. H. Dispersion and Absorption of Structure-Borne Sound in Acoustically Thick Plates, *Applied Acoustics* 41 (1994) 97-111.
4. Ross D. *Mechanics of underwater noise*, Peninsula Publishing Los Altos, California, p. 159 (1987).
5. Roelens I., Nuytten F., Bosmans I. and Vermeir G. In Situ Measurement Of The Stiffness Properties Of Building Components. *Applied Acoustics*, 1997, Vol. 52 n°.3/4, 289-309.
6. Craik R. J. M. The measurement of the material properties of building structures, *Applied Acoustics* 15 (1982) 275-282.
7. Young-Chul C., Doo-Byung Y., Jin-Ho P. and Hyu-Sang Kwon. An In-situ Young's Modulus Measurement Technique For Nuclear Power Plants Using Time-Frequency Analysis. *Nuclear engineering and technology*, 2009, Vol.41 n°.3, 327-334.
8. Mecking S., Schanda U., Schoenwald S. Material characterisation of Cross Laminated Timber using experimental wave velocities, *Proceedings, Euronoise 2018, Crete*.
9. Biurrun Manresa J. The Wigner-Ville Distribution, Lecture 2. Aalborg University 2011.